ChemComm
Chemical Communications

Accepted Manuscript

This article can be cited before page numbers have been issued, to do this please use: E. Procházková, P. Šimon, M. Straka, J. Filo, M. Majek, M. Cigá and O. Baszczyski, *Chem. Commun.*, 2020, DOI: 10.1039/D0CC06928K.

ROYAL SOCIETY OF CHEMISTRY

rsc.li/chemcomm

View Article Online
DOI: 10.1039/D0CC06928K

COMMUNICATION

Phosphate Linkers with Traceable Cyclic Intermediates for Self-Immolation Detection and Monitoring

Eliška Procházková,[a] Petr Šimon,[b] Michal Straka,[a] Juraj Filo,[c] Michal Májek,[c] Marek Cigáň [c] and Ondřej Baszczyňski[b,*]

Received 00th January 20xx,
Accepted 00th January 20xx

DOI: 10.1039/x0xx00000x

Self-immolation (SI) is the key principle of ProTide nucleotide prodrugs such as remdesivir, which is currently used to treat COVID-19 patients. Developing of novel tailor-made SI systems requires new analytical methods for detection and monitoring the SI. We developed a robust method for SI analysis using novel phosphate-based SI linkers with NMR traceable cyclic intermediates to distinguish SI from alternative fragmentation pathways and to monitor cargo release in real time.

Self-immolative (SI) linkers are subjected to irreversible fragmentation initiated by an external trigger and can be used to develop smart materials (*e.g.,* degradable polymers) or drug delivery systems.[1,2] In principle, the activated linker forms a cyclic intermediate, which tends to release the leaving group (cargo).[3,4] Accordingly, phosphate-based SI linkers are more versatile than their carbon analogues because phosphorus has a higher valency (V) than carbon (IV), thus enabling an additional substituent.[5–7]

SI processes are typically monitored by optical spectroscopy using chromogenic/fluorogenic substrates.[8] This approach is versatile and easy to use, *e.g.,* in high-throughput screenings of structurally similar derivatives. However, optical spectroscopy provides only limited data on complex reaction sequences. This limited knowledge may lead to misinterpretation of spectral data. In addition, SI itself has other drawbacks: 1) Enzymatic activation of SI may alter the SI process as a result of substrate specificity,[9] and chemical activation requires carefully handling chemical precursors and controlling both temperature and activation time. 2) For each chromogenic/fluorogenic moiety, the assay must be re-optimised. 3) Colourless leaving groups cannot be monitored directly. To overcome these obstacles, we recently proposed photo-activated, phosphate-based SI linkers for reaction monitoring by ^{31}P NMR spectroscopy. Our approach provides both kinetic and structural data and can be used as a diagnostic tool for screening newly developed SI linkers.[10,11]

Here, we present another advancement involving phosphate-based SI linkers, more specifically, the development of a new method for detecting and monitoring SI processes based on cyclic phosphate intermediates, which are stable enough for direct NMR detection. This method allows us to clearly differentiate self-immolation from other processes, such as hydrolysis or alternative decomposition with undesired side-products, and thereby overcoming the limitations of optical spectroscopy monitoring.

We propose the following SI mechanism for the newly designed linkers **1**–**6**: a) photoactivation, cleavage of the photo-removable dimethoxy nitrobenzyl (DMNB) moiety and fast release of CO_2, yielding the activated intermediate **I**, b) self-immolation: cyclisation and cargo release, affording the cyclic intermediate **cyc-I**, and c) spontaneous **cyc-I** ring-opening, providing the final product **P** (Fig. 1). To enhance the functionality of our method, we used the most promising ethylene glycol linker in compound **2** (X, Y = O) to study cargo release in derivatives **7**–**10**.

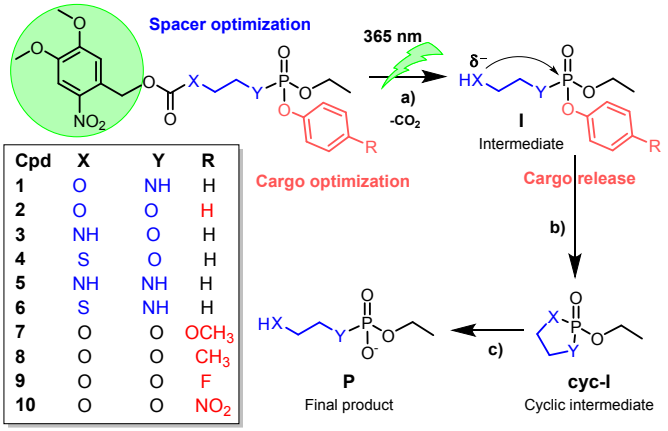

Cpd	X	Y	R
1	O	NH	H
2	O	O	H
3	NH	O	H
4	S	O	H
5	NH	NH	H
6	S	NH	H
7	O	O	OCH_3
8	O	O	CH_3
9	O	O	F
10	O	O	NO_2

Fig. 1 Chemical structure of phosphate-based linkers **1**–**10** studied in this work and the proposed mechanism of self-immolation; a) photoactivation, and CO_2 release; b) cyclisation, and cargo release; c) cyclic intermediate **cyc-I** ring opening.

[a] *Institute of Organic Chemistry and Biochemistry, Czech Academy of Sciences, Prague 166 10, Czech Republic*
[b] *Faculty of Science, Charles University, Prague 128 43, Czech Republic*
[c] *Department of Organic Chemistry, Faculty of Natural Sciences, Comenius University, Bratislava 842 15, Slovakia.*
† Footnotes relating to the title and/or authors should appear here.
Electronic Supplementary Information (ESI) available: [details of any supplementary information available should be included here]. See DOI: 10.1039/x0xx00000x

The SI reactions of **1–6** were monitored by ^{31}P NMR spectroscopy, upon continuous irradiation, which revealed alterations. Based on the results, these reactions were divided into three main classes: a) Successful SI process with phenol release (**1**, **2**), b) spacer self-cleavage without phenol release (**3**, **4**) and, c) photoactivation with no further reaction (**5**, **6**).

Self-immolation of **1** and **2** (Figs. 2A and 2B, respectively) followed the proposed reaction pathway (Fig. 1). Photoactivation of **1** (δ_P +5.8 ppm) and **2** (δ_P –6.5 ppm) provided the corresponding intermediates **1-I and 2-I** (δ_P +6.3 and –6.1 ppm, respectively), which consequently formed the cyclic intermediate **cyc-I**, as detected in ^{31}P spectra[14] (26.9 and 18.1 ppm, respectively). Interestingly, **2-cyc-I** was formed ca. four times faster than **1-cyc-I**, thus yielding the final product **2-P** in 90 minutes, while **1-P** was formed overnight (Fig. S7 in the ESI). The detection of the cyclic intermediate clearly confirms that both compounds **1** and **2** release phenol by self-immolation (Figs. S7–S11 in the ESI). More importantly, the presence of cyclic intermediates could not be detected by optical spectroscopy, the conventionally used method.

Surprisingly, compounds **3** and **4**, as single-atom alterations of **2**, where X=O is substituted by NH and S, respectively, provided no cyclic intermediate or the desired final product **P** (Figs. 2C and 2D, respectively). Moreover, an identical side product, **sideP** (δ_P –5.4 ppm), was detected in both cases (Figs. S12–S13 in the ESI), indicating that the spacer was released instead of the phenol. For **3**, this result can be explained by the inability of the spacer to cyclise due to protonation of the terminal NH_2. Instead, the system undergoes simple chemical hydrolysis of the spacer. For **4**, we assume self-cleavage of the thiol spacer through a known thiirane mechanism.[15,16] Spacer self-cleavage may find its application in the design of phosphorylating agents (*e.g.,* amino acid or protein phosphorylation) and antiviral prodrugs (*e.g.,* ProTides concept).[17–21] Note, however, that no spacer self-cleavage was observed in either **1** or **2**.

Compounds **5** and **6** formed intermediates **5-I** and **6-I** upon photoactivation, with no further spectral change (Fig. S14 in the SI).

To demonstrate the practical use of the proposed method, we selected the ethylene glycol linker used in **2** as the best candidate for a more detailed mechanistic study of cargo release. We prepared derivatives **7–10** differing in *para*-substituents on the phenyl ring (Fig. 1). In all cases, the *para*-substituted phenol was released by SI upon irradiation, as indicated by the formation of **2-cyc-I** (18.1 ppm), (Fig. S15 in the ESI). As expected, *para*-substitution had a strong effect on the cyclisation rate, as shown by the formation of the corresponding intermediates **I** (Table 1). Compounds **7** and **8**, with the electron-donating OCH_3 and CH_3, respectively, had slower cyclisation rates than **9** and **10** and provided the highest concentrations of **I** (ca. 35 % in 30 min. of irradiation). The results have also highlighted a strong correlation between Hammett constants, the pK_a of the corresponding phenols (leaving groups), and the general ability of **I** to cyclise. The better the leaving group was (in **10** with the electron-withdrawing NO_2 group with σ_p=0.81 and pK_a=7.15), the lower the concentration of the intermediate $[\mathbf{I}]_{rel}$ and, accordingly, the faster the cyclisation and cargo release were (Table 1). Importantly, slow spontaneous hydrolysis of **10** could be easily misinterpreted for self-immolation, especially when using optical spectroscopy, because both reaction mixtures become yellow (Fig. 3).

To test whether photo-activation would account for any discrepancies in our study, we checked the photochemical activation rates of **1–6**, which were comparable within the series (same order of magnitude), while the photolysis quantum yields (QYs) of derivatives **3** and **5** differed slightly (Table S1 in the ESI). Therefore, we performed a computational study to assess this effect (Fig. 4 and ESI Section 2). Based on the literature, we expected a correlation between the experimentally obtained QYs and the calculated activation energy $\Delta G_{(TS\text{-}S1)}$ of excited-state hydrogen transfer (ESHT) in the first singlet excited state S_1.[22]

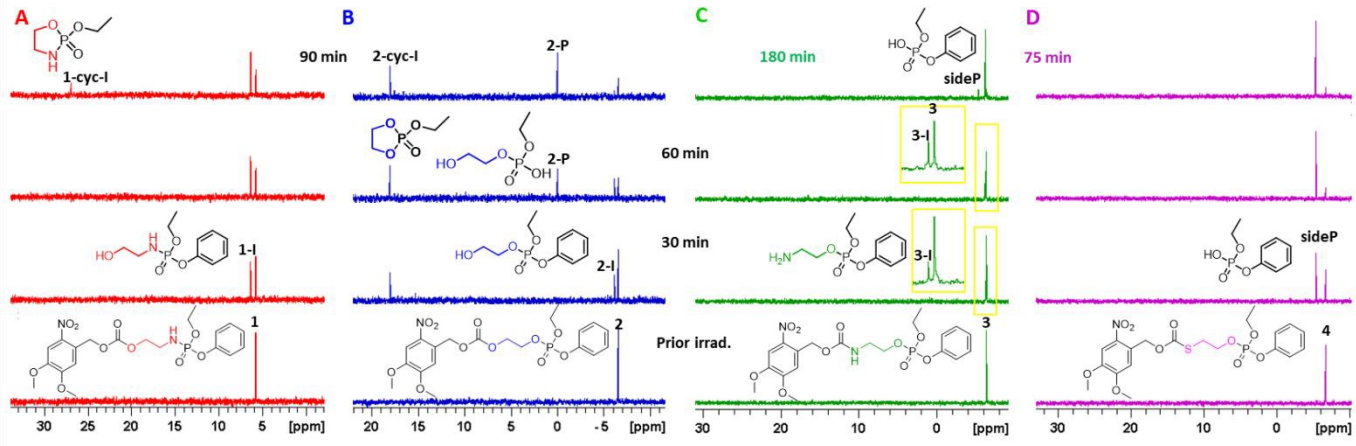

Fig. 2 A series of ^{31}P NMR spectra of compounds **1–4** and their derivatives in 50% CACO*/DMSO (0.5 mM) recorded upon continuous irradiation by UV light (365 nm) at room temperature. The patterns for compounds **5** and **6**, where intermediates **5-I** and **6-I** do not provide any further reaction, are shown in ESI (Fig. S14). * CACO = cacodylate buffer (0.1 M, pH 7.4).

View Article Online
DOI: 10.1039/D0CC06928K

Table 1 Effect of *para*-substituents on the rate of cargo release

Cpd	R	σ_p[26]	pK_a[a]	δ ^{31}p[b] (ppm)	$[I]_{rel}^{30min.}$
2	H	0	9.98[27]	–6.52	0.31
7	OCH_3	–0.28	10.55[28]	–6.11	0.34
8	CH_3	–0.14	10.14[27]	–6.37	0.36
9	F	0.15	9.95[29]	–6.43	0.16
10	NO_2	0.81	7.15[27]	–7.51	0[c]

[a] pKa values of *para*-substituted phenol which is cleaved off by SI process. [b] Measured as 0.5 mM solution in 50% CACO/DMSO at room temperature. [c] The formed intermediate **10-I** is immediately and quantitatively converted into the cyclic intermediate **2-cyc-I**.

For compounds **1**, **2** and **4**, **6** (X = O and S, respectively), the height of the barrier in S_1 was effectively the same ($\Delta G_{(TS\text{-}S1)}$ = 8.4 and 8.3 kcal/mol, respectively), which indicates similar reactivity and corresponds to the determined QYs. The QYs of these four compounds ranged from 0.003 to 0.009, in line with previously reported values for a similar compound with a slightly lower barrier of 7.8 kcal/mol translated to a QY of 0.008.[22,23] In turn, the predicted activation energy $\Delta G_{(TS\text{-}S1)}$ of compounds **3** and **5** (X = N) was 7.3 kcal/mol, which explains the slightly higher QYs (0.019 and 0.016, respectively).

Intersystem crossing (ISC) into the triplet state T_2 was also considered. We calculated a spin orbit coupling of 38 cm^{-1}, the same value for all three model groups (X = O, S and NH; Fig. 4). This is approximately half of the value reported for the simple *o*-nitrotoluene derivatives.[22] Therefore, we hypothesize that ISC is less important in our compounds **1**–**6** than in the previously reported *o*-nitrobenzenes (details in ESI) and that the difference in reactivit y between the O/S and N-bearing compounds primarily results from the difference in activation energy at the S_1 singlet excited state (ΔG(TS-S_1)).

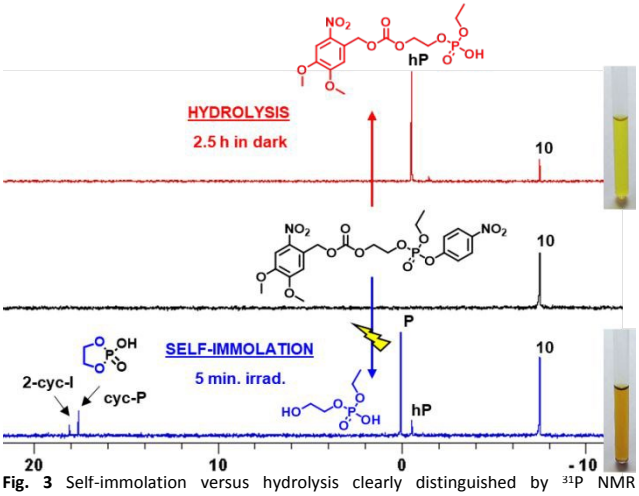

Fig. 3 Self-immolation versus hydrolysis clearly distinguished by ^{31}P NMR spectroscopy. Detection of the cyclic products **cyc-I** and **cyc-P** provides direct evidence of self-immolation, which could not be obtained when using optical methods.

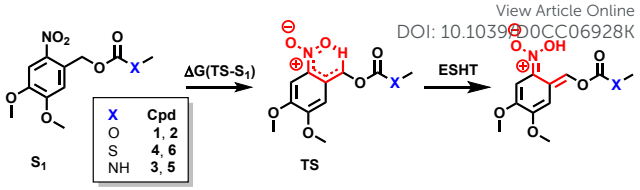

Fig. 4 The transition state structures proposed for the photoactivation step. For simplicity, the "ethylene glycol" spacers were substituted by a methyl group.

For further insight into the self-immolation of **1** and **2**, DFT calculations were performed. The reaction pathway was pre-constructed based on previous studies.[10,24] The corresponding reactants, products, and intermediates were minimised and interconnected by optimised transition states, as described in ESI in detail. The following mechanism was proposed.

After the initiation, the photosensitive DMNB moiety is cleaved off, and fast CO_2 release provides intermediate **I.**[13] The proposed structure of intermediate **I** is supported by the calculated ^{31}P NMR chemical shifts (Table S2 in ESI), which differ from those with a carbonate/carbamate system. **I** then deprotonates to **(I-H)**$^-$, which is able to attack the central P atom whilst forming a cyclic intermediate **cyc-I(OPh)** via **TS1**, as shown in Fig. 5. The predicted barrier for this process is 32.5 (23.1) kcal/mol for **1** (**2**), respectively. This barrier includes an energy penalty for **I-OH** deprotonation of 28 and 21 kcal/mol for **1** (**2**) estimated from the calculated pK_a of **1** (**2**) (ESI). The barrier is lower for **1** than for **2** (Fig. 5), which qualitatively explains why the SI process is much faster for **1** (see above). The intermediate **cyc-I(OPh)** lies approximately 7 kcal/mol under the pre-reaction complex and rapidly cleaves the phenolate group – this process has a barrier of only 1.9 (2.0) kcal/mol for **1** (**2**) (see **TS2** in Fig. 5). For this reason, the **cyc-I(OPh)** intermediate (Fig. 5) could be observed in gas-phase IRPD studies[10] but not in the solution-state NMR experiments performed here. The resulting stable **cyc-I** intermediate was detected in NMR experiments (Figs. 2 and 3 and Table S1 in ESI). Overall, the SI process is exothermic (Fig. 5). [25]

In conclusion, we introduced a new practical and straightforward method for SI detection. For this purpose, we designed novel SI linkers, which form cyclic intermediates detectable by NMR spectroscopy. We have shown that self-immolation on phosphate-based linkers is highly sensitive to the phosphorus environment, particularly to both ends of the activated SI linker. As such, the attacking end should have a high affinity to phosphorus. In addition, the cargo release rate is significantly affected by the pK_a of the cargo itself. The cyclic intermediates are easy to monitor by NMR spectroscopy, thus enabling us to differentiate self–immolation from hydrolysis and/or detect the formation of side products, which could possibly alter the SI reaction. Ultimately, this approach and our linkers will pave the way to design novel SI constructs useful in Medicine (e.g., antiviral prodrugs – new phosphoramidate ProTide analogues) and Materials Science (e.g., self-degradable smart polymers).

View Article Online
DOI: 10.1039/D0CC06928K

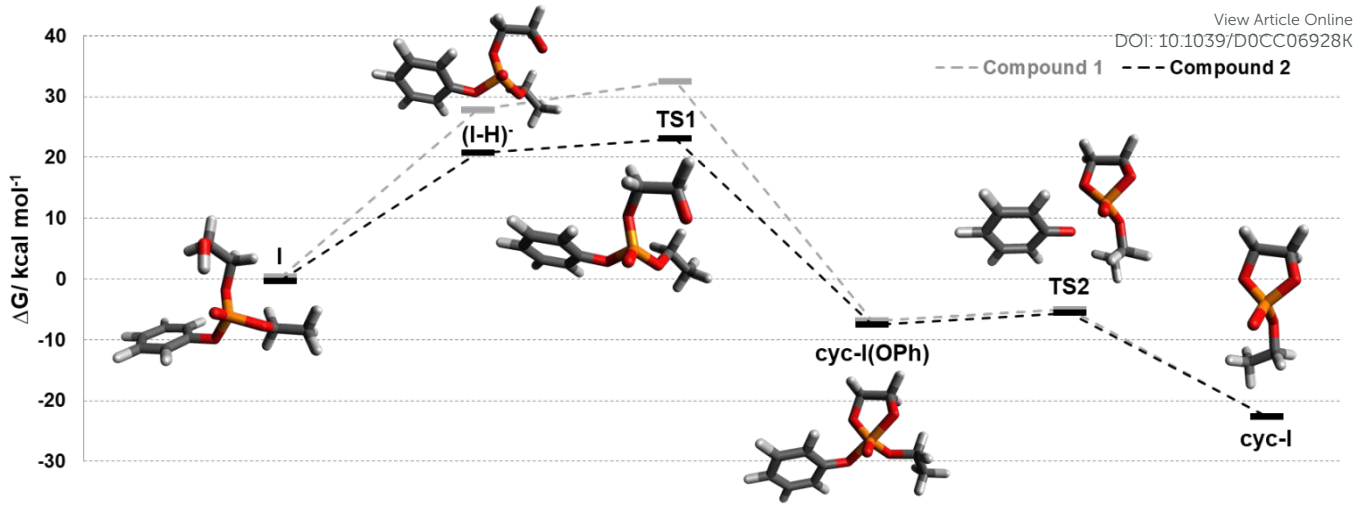

Fig. 5 Mechanism of the self-immolation of **2** proposed by DFT calculations using B3LYP/def2TZVP level in implicit solvent water, see ESI. As an example, the optimised structures of compound **2** corresponding to energy profile in black are shown. An energy profile of compound **1** is shown in grey.

This work was supported by the Experientia Foundation (O.B., Start-Up grant SG-2018-1), the Czech Science Foundation (O.B., grant No. 20-25137Y), and the Slovak Research and Development Agency (M.C., grant APVV-15-0495). We thank Dr. Ondřej Gutten for calculation the pK_a constants. We would also like to acknowledge Květoslava Kertisová and Kateřina Nováková, from the Mass Spectroscopy Department at IOCB, for the HR-MS spectra, and we thank Dr. Carlos V. Melo for editing the manuscript.

Conflicts of interest

There are no conflicts to declare.

Notes and references

1 A. Alouane, R. Labruère, T. Le Saux, F. Schmidt and L. Jullien, *Angew. Chemie - Int. Ed.*, 2015, **54**, 7492–7509.
2 A. Sagi, R. Weinstain, N. Karton, and D. Shabat *J. Am. Chem. Soc.*, 2008, **130**, 5434–5435.
3 J. Yan, S. Lee, A. Zhang and J. Yoon, *Chem. Soc. Rev.*, 2018, **47**, 6900–6916.
4 A. D. Wong, M. A. DeWit, and E. R. Gillies, *Adv. Drug Deliv. Rev.*, 2012, **64**, 1031–1045.
5 A. S. Alanazi, E. James, and Y. Mehellou, *ACS Med. Chem. Lett.*, 2019, **10**, 2–5.
6 Y. Wei, G. Qiu, B. Lei, L. Qin, H. Chu, Y. Lu, G. Zhu, Q. Gao, Q. Huang, G. Qian, P. Liao, X. Luo, X. Zhang, C. Zhang, Y. Li, S. Zheng, Y. Yu, P. Tang, J. Ni, P. Yan, Y. Zhou, P. Li, X. Huang, A. Gong, and J. Liu, *J. Med. Chem.*, 2017, **60**, 8580–8590.
7 A. M. Caminade, *Chem. Commun.*, 2017, **53**, 9830–9838.
8 S. Gnaim and D. Shabat, *Acc. Chem. Res.*, 2019, **52**, 2806–2817.
9 E. Procházková, H. Hřebabecký, M. Dejmek, M. Šála, M. Šmídková, E. Tloušťová, E. Zborníková, L. Eyer, D. Růžek, and R. Nencka, *Bioorg. Med. Chem. Lett.*, 2020, **30**, 126897, 1–4.
10 E. Procházková, R. Navrátil, Z. Janeba, J. Roithová, and O. Baszczyňski, *Org. Biomol. Chem.*, 2019, **17**, 315–320.
11 E. Procházková, J. Filo, M. Cigáň and O. Baszczyňski, *Eur. J. Org. Chem.*, 2020, **7**, 897–906.
12 I. Aujard, C. Benbrahim, M. Gouget, O. Ruel, J. B. Baudin, P. Neveu and L. Jullien, *Chem. - A Eur. J.*, 2006, **12**, 6865–6879.
13 P. Klán, T. Šolomek, C. G. Bochet, A. Blanc, R. Givens, M. Rubina, V. Popik, A. Kostikov, and J. Wirz, *Chem. Rev.*, 2013, **113**, 119–191.
14 L. K. Müller, T. Steinbach and F. R. Wurm, *RSC Adv.*, 2015, **5**, 42881–42888.
15 M. Shafiee, S. Deferme, A. -L. Villard, D. Egron, G. Gosselin, J. L. Imbach, T. Lioux, A. Pompon, S. Varray, A. M. Aubertin, G. V. Den Mooter, R. Kinget, C. Périgaud and P. Augustijns, *J. Pharm. Sci.*, 2001, **90**, 448–463.
16 U. Pradere, E. C. Garnier-Amblard, S. J. Coats, F. Amblard and R. F. Schinazi, *Chem. Rev.*, 2014, **114**, 9154–9218.
17 M. Samarasimhareddy, G. Mayer, M. Hurevich and A. Friedler, *Org. Biomol. Chem.*, 2020, **18**, 3405–3422.
18 A. Hauser, M. Penkert and C. P. R. Hackenberger, *Acc. Chem. Res.*, 2017, **50**, 1883–1893.
19 K. D. Siebertz and C. P. R. Hackenberger, *Chem. Commun.*, 2018, **54**, 763–766.
20 M. Slusarczyk, M. H. Lopez, J. Balzarini, M. Mason, W. G. Jiang, S. Blagden, E. Thompson, E. Ghazaly and C. McGuigan, *J. Med. Chem.*, 2014, **57**, 1531–1542.
21 Y. Mehellou, H. S. Rattan and J. Balzarini, *J. Med. Chem.*, 2018, **61**, 2211–2226.
22 T. Šolomek, C. G. Bochet and T. Bally, *Chem. - A Eur. J.*, 2014, **20**, 8062–8067.
23 T. Šolomek, S. Mercier, T. Bally and C. G. Bochet, *Photochem. Photobiol. Sci.*, 2012, **11**, 548–555.
24 A. Ricci and A. Brancale, *J. Comput. Chem.*, 2012, **33**, 1029–1037.
25 P. Gillespie, F. Ramirez, I. Ugi and D. Marquarding, *Angew. Chem. Int. Ed. Engl.*, 1973, **12**, 91–172.
26 *Org. Process Res. Dev.*, 2001, **5**, 669–669.
27 I. Sharma and G. A. Kaminski, *J. Comput. Chem.*, 2012, **33**, 2388–2399.
28 G. Chuchani and A. Frohlich, *J. Chem. Soc. B Phys. Org.*, 1971, **78**, 1417–1420.
29 K. Roy and P. L. A. Popelier, *J. Phys. Org. Chem.*, 2009, **22**, 186–196.